

HETEROCYCLES, Vol. 86, No. 2, 2012, pp. 991 - 996. © 2012 The Japan Institute of Heterocyclic Chemistry
Received, 10th August, 2012, Accepted, 25th September, 2012, Published online, 5th October, 2012
DOI: 10.3987/COM-12-S(N)107

ISOLATION AND FIRST X-RAY STRUCTURES OF NICKEL COMPLEXES OF 1,2,5-THIADIAZOLE-3,4-DITHIOLATE (TDAS) IN PROTONATED FORMS

Kouzou Matsumoto,* Maho Nishizawa, Yasukazu Hirao, Hiroyuki Kurata, and Takashi Kubo*

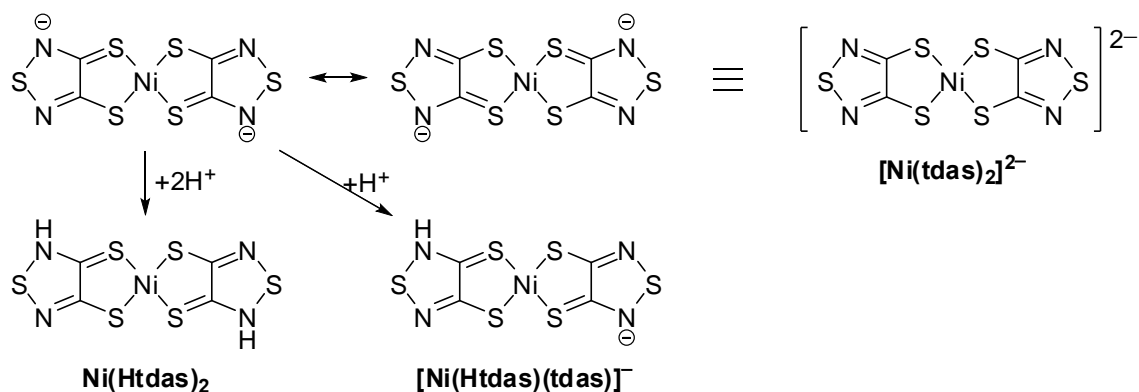
Department of Chemistry, Graduate School of Science, Osaka University, 1-1 Machikaneyama, Toyonaka, Osaka 560-0043, Japan

E-mail: matsumoto@isc.senshu-u.ac.jp, kubo@chem.sci.osaka-u.ac.jp

Dedicated to Professor Ei-ichi Negishi on the occasion of his 77th birthday

Abstract – Protonated Ni(tdas)₂ complexes, tdas = 1,2,5-thiadiazole-3,4-dithiolate, are isolated and characterized by X-ray crystallography. pH-Dependent absorption measurements reveal high proton donor ability of Ni(Htdas)₂.

Metal bis(dithiolene) complexes have attracted intense interest as electro-conductive and magnetic materials.¹ Within the family of dithiolene ligands 1,3-dithiole-2-thione-4,5-dithiolato (dmit), maleonitrile-2,3-dithiolato (mnt), and 5,6-dihydro-1,4-dithiin-2,3-dithiolate (dddt) are widely used. The 1,2,5-thiadiazole-3,4-dithiolate (tdas) ligand has been also intensively studied as M(tdas)₂ complexes (M = Ni, Pd, Pt, Fe, Co, Cu, Au) in terms of potential application of functional materials^{2,3} since the first isolation as a nickel complex.^{2a} The tdas ligand possesses an electron-deficient heteroaromatic ring, and consequently, stable redox states of M(tdas)₂ are dianion and monoanion states, while a neutral state appears to be difficult to generate according to the cyclic voltammogram that shows the irreversible anodic wave during [Ni(tdas)₂]⁻ → [Ni(tdas)₂]⁰ oxidation process.²ⁱ Indeed the neutral complex of M(tdas)₂ has not been isolated yet. Therefore, the use of M(tdas)₂ has been limited to anion counterparts of charge transfer complexes or salts. On the other hand, the tdas ligand should exist in a protonated form as shown in Scheme 1, which could lead to a neutral form of the M(tdas)₂ systems. This not only expands the possibility of M(tdas)₂ for electro-conductive and magnetic materials, but also leads to a new function such as ferroelectricity⁴ because a protonated M(tdas)₂ is expected to behave as a good proton donor. Herein we report the first isolation and characterization of protonated Ni(tdas)₂ complexes.



Scheme 1. Dianion and protonated states of Ni(tdas)₂

In order to obtain protonated tdas metal complexes, we thoroughly investigated the protonation of $[\text{Ni}(\text{tdas})_2]^{2-}$.^{2b} After many trials, we could find the appropriate reaction conditions that a di-protonated complex Ni(Htdas)₂ and a mono-protonated complex $[\text{Ni}(\text{Htdas})(\text{tdas})]^-$ can be selectively obtained by changing the counter ions of $[\text{Ni}(\text{tdas})_2]^{2-}$. For the di-protonated complex Ni(Htdas)₂, trifluoroacetic acid (TFA) was added to a solution of $(\text{Et}_4\text{N})_2[\text{Ni}(\text{tdas})_2]$ in acetonitrile.⁵ Ni(Htdas)₂ was obtained as a deep purple solid. Elemental analysis and IR measurement of the solid fully supported the exclusive formation of di-protonated species. Single crystals of Ni(Htdas)₂ suitable for X-ray crystallographic analysis were obtained by the addition of concentrated nitric acid to an aqueous solution of $(\text{Et}_4\text{N})_2[\text{Ni}(\text{tdas})_2]$. Other recrystallization conditions (TFA or hydrochloric acid in acetonitrile, water, or *N,N*-dimethylformamide) gave only a microcrystalline solid or decomposed products. The mono-protonated complex $(n\text{-Bu}_4\text{N})[\text{Ni}(\text{Htdas})(\text{tdas})]$ was obtained as red prisms by the addition of TFA into an acetonitrile solution of $(n\text{-Bu}_4\text{N})_2[\text{Ni}(\text{tdas})_2]$.⁶ The selective formation of $(n\text{-Bu}_4\text{N})[\text{Ni}(\text{Htdas})(\text{tdas})]$ is due to the lower solubility of $(n\text{-Bu}_4\text{N})[\text{Ni}(\text{Htdas})(\text{tdas})]$ than Ni(Htdas)₂ in acetonitrile. Elemental analysis and IR measurement of the red prisms supported the selective formation of mono-protonated species.

The X-ray structure of Ni(Htdas)₂ is shown in Figure 1.⁷ Ni(Htdas)₂ forms a N–H···O hydrogen bond (2.721 Å) with a water molecule (Figure 1a). Contrary to the planar structure of $[\text{Ni}(\text{tdas})_2]^{2-}$,^{2b,2d,2e,2f,2h,2i,2k-n} Ni(Htdas)₂ takes a “Z-shaped” structure (Figure 1b). The dihedral angle between the mean plane of Htdas and the central NiS₄ plane is approximately 12.0°. There are some differences in bond lengths between Ni(Htdas)₂ and $[\text{Ni}(\text{tdas})_2]^{2-}$. The bond lengths of S2–C2 (1.698 (7) Å) and N2–C2 (1.333(8) Å) of Ni(Htdas)₂ are shorter and longer than the corresponding bonds of $[\text{Ni}(\text{tdas})_2]^{2-}$,⁸ due to their double and single bond character (see, Scheme 1), respectively. In crystal, Ni(Htdas)₂ molecules stack along the *a*-axis and the stack columns are connected by hydrogen bonds with water molecules and by short S···S contacts between neighboring molecules (S2···S3; 3.175 Å, S1···S3; 3.341 Å).

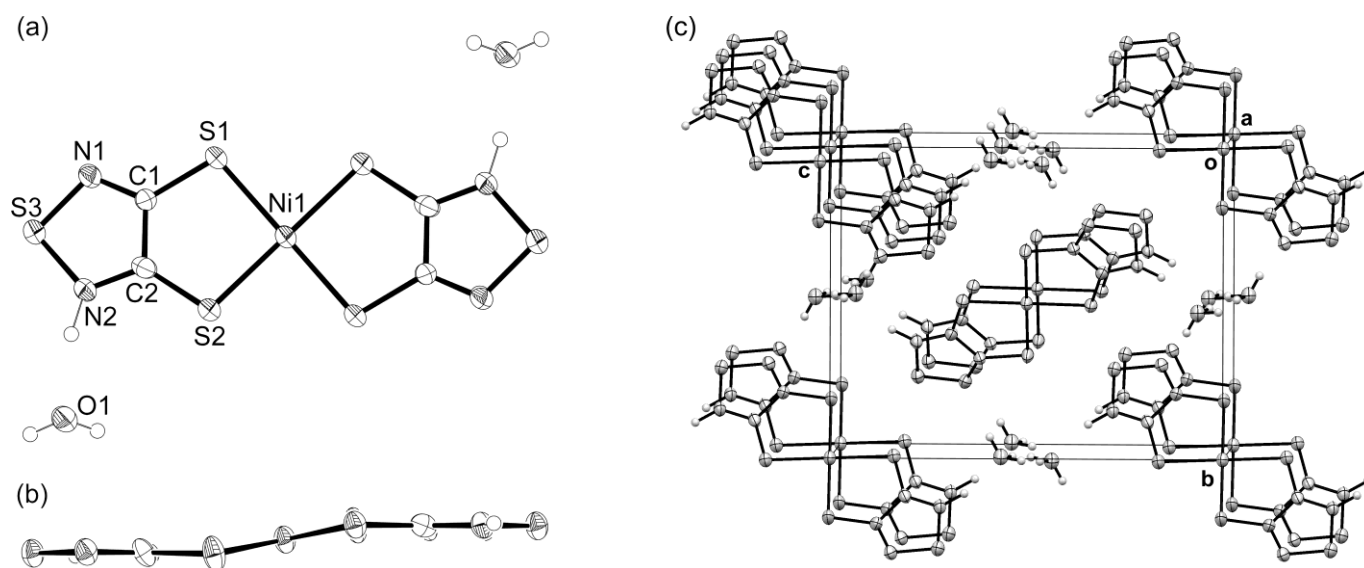


Figure 1. ORTEP drawings of $\text{Ni}(\text{Htdas})_2$. (a) Top view, (b) side view, and (c) packing diagram.

Figure 2 shows the X-ray structure of $(n\text{-Bu}_4\text{N})[\text{Ni}(\text{Htdas})(\text{tdas})]$.⁹ There are two crystallographically independent $(n\text{-Bu}_4\text{N})[\text{Ni}(\text{Htdas})(\text{tdas})]$ molecules in the unit cell. Although the high R_1 -value (8.8%) prohibits detailed discussion on molecular geometries, both $[\text{Ni}(\text{Htdas})(\text{tdas})]^-$ takes almost similar structure with high planarity (Figure 2b). $[\text{Ni}(\text{Htdas})(\text{tdas})]^-$ forms a one-dimensional (1D) chain running along the $[1\ -1\ 0]$ direction (Figure 2c) through the $\text{N}\cdots\text{H}\cdots\text{N}$ hydrogen bonds ($\text{N}2\cdots\text{N}6$; 2.733 Å and $\text{N}4\cdots\text{N}8$; 2.745 Å) between neighboring molecules. Short $\text{S}\cdots\text{S}$ contacts ($\text{S}2\cdots\text{S}9$; 3.335 Å and $\text{S}5\cdots\text{S}12$; 3.379 Å) were observed in the 1D chain, while there was no appreciable short $\text{S}\cdots\text{S}$ contact between the 1D chains. The sheet of $[\text{Ni}(\text{Htdas})(\text{tdas})]^-$ and that of tetrabutylammonium ion stack alternately along the c axis (Figure 3a).

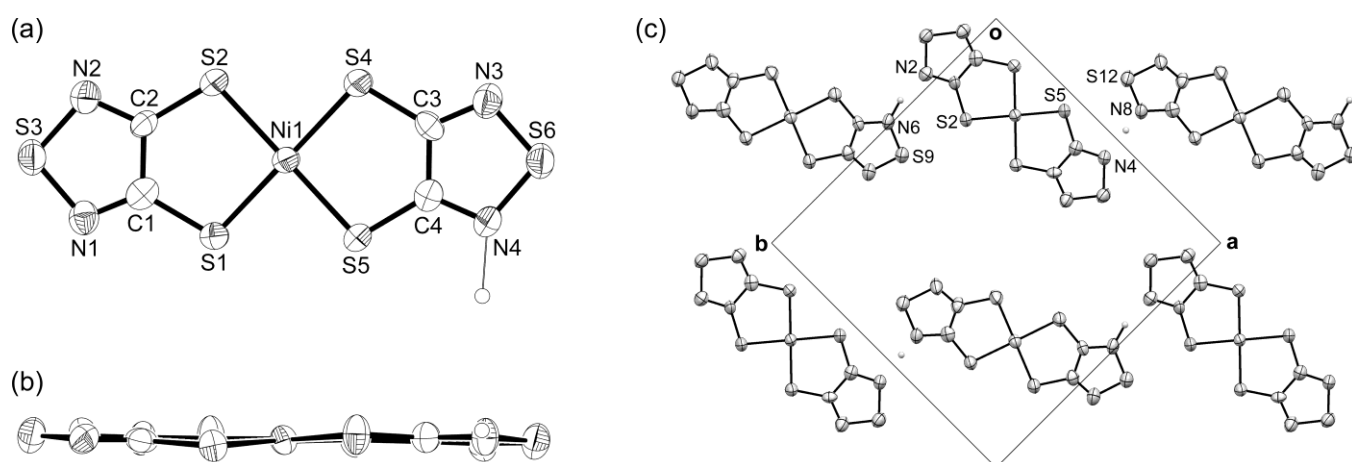


Figure 2. ORTEP drawings of $(n\text{-Bu}_4\text{N})[\text{Ni}(\text{Htdas})(\text{tdas})]$. (a) Top view and (b) side view of $[\text{Ni}(\text{Htdas})(\text{tdas})]^-$ (one of the crystallographically independent molecules is shown), and (c) molecular arrangement of $[\text{Ni}(\text{Htdas})(\text{tdas})]^-$ in a $(0\ 0\ 1)$ plane.

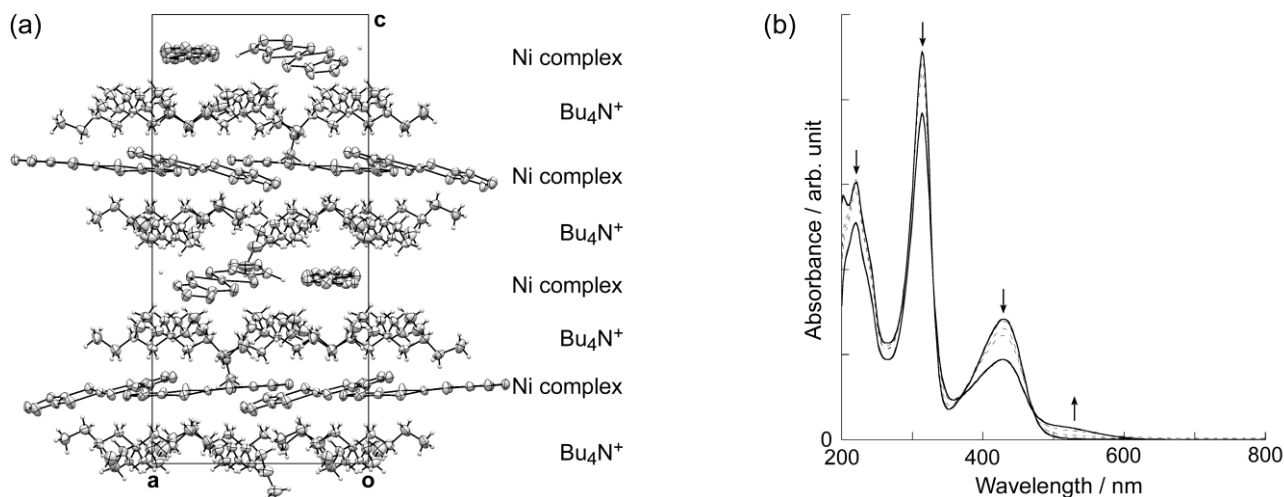
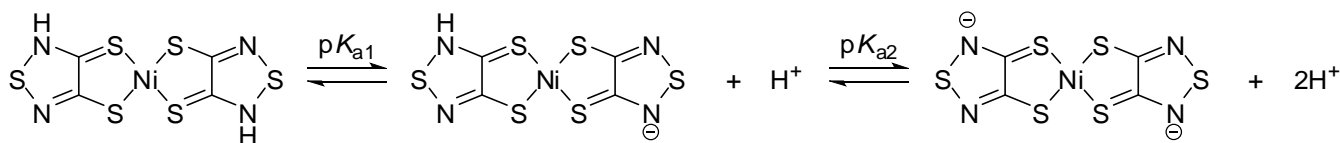


Figure 3. (a) Crystal packing of $(n\text{-Bu}_4\text{N})[\text{Ni}(\text{Htdas})(\text{tdas})]$ along the b -axis. (b) pH dependent absorption spectra of $(n\text{-Bu}_4\text{N})_2[\text{Ni}(\text{tdas})_2]$ in an acetonitrile–water solution ($v/v = 1:1$) at room temperature. The absorption at 416 nm was decreased with decreasing the pH of the solution. The pH values measured are 5.51, 1.56, 0.82, 0.50, and 0.13. The weak shoulder-like absorption in the 500–600 nm range is attributable to $[\text{Ni}(\text{Htdas})(\text{tdas})]^-$.

As mentioned above, $\text{Ni}(\text{Htdas})_2$ is expected to behave as a good proton donor. In order to estimate the pK_a values of $\text{Ni}(\text{Htdas})_2$ (Scheme 2), pH dependent absorption spectra of $(n\text{-Bu}_4\text{N})_2[\text{Ni}(\text{tdas})_2]$ were measured (Figure 3b).¹⁰ However, the pK_a values of $\text{Ni}(\text{Htdas})_2$ could not be determined because the absorption bands of $[\text{Ni}(\text{tdas})_2]^{2-}$ did not completely disappear even when the pH of the solution was nearly zero. This result indicates that the $\text{Ni}(\text{Htdas})_2$ possesses the pK_a values of less than zero and accordingly prominent proton donor ability.



Scheme 2. Proton dissociation process of $\text{Ni}(\text{Htdas})_2$

In summary, we isolated nickel complexes with tdas ligands in protonated forms. $\text{Ni}(\text{Htdas})_2$ and $[\text{Ni}(\text{Htdas})(\text{tdas})]^-$ possess high proton donor ability due to the electron deficiency of the thiadiazole ring. Investigation on functional properties of $\text{Ni}(\text{Htdas})_2$ such as electro-conductivity and dielectricity are now in progress in our group.

ACKNOWLEDGEMENTS

This work was supported by a grant from the Iketani Science and Technology Foundation (0201096-A).

REFERENCES AND NOTES

1. N. Robertson and L. Cronin, *Coord. Chem. Rev.*, 2002, **227**, 93.
2. (a) I. Hawkins and A. E. Underhill, *J. Chem. Soc., Chem. Commun.*, 1990, 1593; (b) O. A. Dyachenko, S. V. Konovalikhin, A. I. Kotov, G. V. Shilov, E. B. Yagubskii, C. Faulmann, and P. Cassoux, *J. Chem. Soc., Chem. Commun.*, 1993, 508; (c) S. Schenk, I. Hawkins, S. B. Wilkes, A. E. Underhill, A. Kobayashi, and H. Kobayashi, *J. Chem. Soc., Chem. Commun.*, 1993, 1648; (d) H. Yamochi, N. Sogoshi, Y. Simizu, G. Saito, and K. Matsumoto, *J. Mater. Chem.*, 2001, **11**, 2216; (e) T. Okuno, K. Kuwamoto, W. Fujita, K. Awaga, and W. Nakanishi, *Polyhedron*, 2003, **22**, 2311; (f) C. Ni, D. Dang, Z. Ni, Y. Li, J. Xie, Q. Meng, and Y. Yao, *J. Coord. Chem.*, 2004, **57**, 1529; (g) S. Curreli, P. Deplano, M. L. Mercuri, L. Pilia, A. Serpe, J. A. Schlueter, M. A. Whited, U. Geiser, E. Coronado, C. J. Gómez-García, and E. Canadell, *Inorg. Chem.*, 2004, **43**, 2049; (h) S. S. Staniland, W. Fujita, Y. Umezono, K. Awaga, S. Crawford, S. Parsons, and N. Robertson, *Mol. Cryst. Liq. Cryst.*, 2006, **452**, 123; (i) M.-G. Liu and C.-L. Ni, *Acta Crystallogr.*, 2006, **E62**, m3039; (j) G. Bruno, M. Almeida, D. Simão, M. L. Mercuri, L. Pilia, A. Serpe, and P. Deplano, *Dalton Trans.*, 2009, 495; (k) H. Zuo, J. Tian, X. Chen, Q. Huang, J.-R. Zhou, X.-P. Liu, C.-L. Ni, and X.-L. Hu, *J. Chem. Crystallogr.*, 2009, **39**, 698; (l) Z.-M. Wang, F.-Q. Wang, and Z.-Y. Liu, *Acta Crystallogr.*, 2011, **E67**, m1143; (m) J.-F. Liu, J. Tian, W.-Q. Chen, L.-B. Liang, L.-L. Yu, L.-M. Yang, J.-R. Zhou, and C.-L. Ni, *J. Chem. Crystallogr.*, 2012, **42**, 450; (n) Z.-H. Zeng and S.-B. Yang, *Acta Crystallogr.*, 2012, **E68**, m239.
3. (a) K. Awaga, T. Okuno, Y. Maruyama, A. Kobayashi, H. Kobayashi, S. Schenk, and A. E. Underhill, *Inorg. Chem.*, 1994, **33**, 5598; (b) N. Robertson, K. Awaga, S. Parsons, A. Kobayashi, and A. E. Underhill, *Adv. Mater. Opt. Electron.*, 1998, **8**, 93; (c) L. Pilia, C. Faulmann, I. Malfant, V. Collière, M. L. Mercuri, P. Deplano, and P. Cassoux, *Acta Crystallogr.*, 2002, **C58**, m240; (d) D. Simão, H. Alves, I. C. Santos, V. Gama, and M. Almeida, *Inorg. Chem. Commun.*, 2003, **6**, 565.
4. S. Horiuchi, Y. Tokunaga, G. Giovannetti, S. Picozzi, H. Itoh, R. Shimano, R. Kumai, and Y. Tokura, *Nature*, 2010, **463**, 789.
5. In a 20 mL flask trifluoroacetic acid (TFA) was added dropwise to a solution of $(\text{Et}_4\text{N})_2[\text{Ni}(\text{tdas})_2]$ (100 mg, 0.12 mmol) in acetonitrile. The solution turned from deep yellow to red. The addition of TFA was continued until the reaction mixture turned reddish purple. Deep purple precipitation appeared and was collected by filtration. Yield: 92% (40 mg). Anal. Calcd for $\text{C}_4\text{H}_2\text{N}_4\text{NiS}_6$: C, 13.45; H, 0.56; N, 15.69. Found: C, 13.68; H, 0.51; N, 15.62. IR (KBr) ν/cm^{-1} 3200–2800mbr, 1435s, 1361s, 1314m, 1198s, 1027w, 1004w, 790s, 767w, 729m, 694m, 675m, 484m.
6. In a 20 mL flask TFA was added to a solution of $(n\text{-Bu}_4\text{N})_2[\text{Ni}(\text{tdas})_2]$ (50 mg, 6.1×10^{-5} mol) in MeCN until the solution turned reddish purple. The red precipitate was collected by filtration. Yield:

83% (30 mg). Anal. Calcd for $C_{20}H_{37}N_5NiS_6$: C, 40.13; H, 6.23; N, 11.70. Found: C, 40.22; H, 6.07; N, 11.64. mp > 100 °C (dec.). IR (KBr) ν/cm^{-1} 2955m, 2928m, 2869m, 2717w, 2634w, 2575w, 2522w, 2354wbr, 1850–1650wbr, 1486w, 1461m, 1395w, 1378s, 1325s, 1231sbr, 1175w, 1149w, 1106w, 1036m, 880w, 798s, 771s, 738w, 700w, 502w, 484w.

7. Crystal data for $Ni(Htdas)_2 \cdot 2H_2O$: $C_4H_6N_4NiO_2S_6$, $M_w = 393.20$, monoclinic, $P2_1/c$ (#14), $a = 4.3660(8)$, $b = 10.7663(17)$, $c = 13.527(3)$ Å, $\beta = 94.051(4)^\circ$, $V = 634.25(19)$ Å³, $T = 200$ K, $Z = 2$, $\rho(\text{calcd}) = 2.059$ g cm⁻³, $\mu(\text{MoK}\alpha) = 2.51$ mm⁻¹, reflections collected = 6130, unique reflections = 1456, $R_{\text{int}} = 0.080$, param. refined = 95, $R1 = 0.054$ ($I > 2\sigma(I)$), $wR2 = 0.149$ (all data), GOF = 1.11. CCDC-901459.
8. According to the reference 2m, the mean bond lengths of S–C and N–C are 1.737 and 1.319 Å, respectively.
9. Crystal data for $(n\text{-Bu}_4\text{N})_2[Ni(\text{tdas})_2]$: $C_{20}H_{37}N_5NiS_6$, $M_w = 598.62$, Tetragonal, $P4_1$ (#76), $a = 14.0423(11)$ Å, $c = 29.073(4)$ Å, $V = 5732.8(10)$ Å³, $T = 150$ K, $Z = 8$, $\rho(\text{calcd}) = 1.385$ g cm⁻³, $\mu(\text{MoK}\alpha) = 1.13$ mm⁻¹, reflections collected = 56984, unique reflections = 13086, $R_{\text{int}} = 0.109$, param. refined = 604, $R1 = 0.088$ ($I > 2\sigma(I)$), $wR2 = 0.223$ (all data), GOF = 1.14. CCDC-901460.
10. Spectrophotometric titrations were carried out with perchloric acid (1 M) in an acetonitrile–water solution ($v/v = 1:1$). The pH measurements were carried out at room temperature using a HORIBA F-12 pH meter.